Astron. Astrophys. 197, 253–260 (1988)

ASTRONOMY
AND
ASTROPHYSICS

CO $J = 2 - 1$ mapping of NGC 1976

Glenn J. White and J. P. Phillips

Physics Department, Queen Mary College, University of London, Mile End Road, London E1 4NS, England

Received March 19, 1987; accepted January 20, 1988

Summary. We present 77 CO $J=2-1$ spectra centred upon four areas about the periphery of the Orion nebula NGC 1976. These reveal evidence of extensive line splitting, with primary components at $V_{LSR} \sim 12\,km\,s^{-1}$ and $V_{LSR} \sim 7\,km\,s^{-1}$. The spatial structure of the regions responsible for these components appears to differ appreciably, and various arguments are outlined to suggest that two distinct segments of a single enveloping cloud are responsible; one to the rear of the H II region ($V_{LSR} \sim 7\,km\,s^{-1}$), associated with various star formation zones, the other in front of NGC 1976, and responsible for localised foregound extinction. This contrasts with previous models, which have proposed compressive shock regions ahead of local ionisation fronts; an hypothesis which is shown not to be necessary, and may be inconsistent with the observed width and conformity of the line splitting zone.

Key words: interstellar medium: molecules – radio lines: molecular – nebulae: Orion nebula

1. Introduction

The extent and mass of the molecular complexes in Orion was first clearly delineated by Kutner et al. (1977), who revealed that two primary concentrations of CO emission were located within Barnard's loop; a northerly component, associated with NGC 2024, NGC 2023, and NGC 2068, and having a typical mass of perhaps $8\ 10^4\,M_\odot$; and a southerly ridge with mass $\sim 10^5\,M_\odot$, containing NGC 1976, NGC 1973, and adjacent star formation zones. Subsequent molecular line mapping has for the most part concentrated about the Kleinmann-Low nebula, a compact area of newly forming stars, characterised by the presence of strong kinematic outflows, shock activity, and high CO temperatures, although a limited number of more extensive investigations have also been undertaken in CO and other molecular line tracers (Gillespie and White, 1980). Loren (1979), for instance, has measured an area ~ 660 arcmin^2 centred upon NGC 1976, revealing several interesting trends between CO line strength and velocity. Where the V_{LSR} is $< 12.6\,km\,s^{-1}$ for instance, it is clear that the primary emission is located towards the OMC-1 star formation region, the dark bay towards the east, and along a narrow ridge extending to the south of NGC 1976. The higher velocity CO emission, on the other hand, appears to define a band or collar of emission which is proximate with the southerly extension of Hβ emission, and is responsible for appreciable line splitting where it overlaps the lower velocity CO component. The additional evidence for strong local [S II] emission from these areas (which may be enhanced in postshock zones (cf. Dopita, 1978)) has been taken to imply shock compression of the ambient material ahead of local ionisation fronts.

Further evidence for this hypothesis is addressed by Schloerb and Loren (1982), who offer a reprise of the Loren (1979) mapping data, together with more limited (but higher resolution) mapping of the OMC-1 core (see also Schloerb et al., 1982), whilst Goldsmith et al. (1982) have published extensive grids of $J=2-1$ ^{13}CO spectra covering a region of size $\sim 100'$, and again overlapping the optical boundaries of NGC 1976. In all of the published spectra, both of ^{13}CO and CO, it is clear that line splitting is strong and highly variable at the nebular boundary, leading to extensive changes of spectral profile over relatively small spatial distances ($\sim 2'$).

2. Observations

In the following, we present a further 77 CO $J=2-1$ spectra taken near the outer boundary of the optical H II region NGC 1976, at the locations indicated in Fig. 1. The results were obtained using the QMC Submillimetre Heterodyne receiver (White et al., 1981; White et al., 1986) mounted on the United Kingdom Infrared Telescope (UKIRT) in Hawaii, and correspond to a beam size 83″, and velocity resolution $1.0\,km\,s^{-1}$. The system noise temperature including atmospheric and telescope losses was 200 K, and quoted temperatures are in units of $T_R^* = T_A^*/\eta_{fss}$, where η_{fss} was determined to be 0.88 at 230 GHz. The spectra were calibrated at ten minute intervals using an ambient chopper vane to remove atmospheric attenuation and telescope losses, whilst atmospheric transmission was found to be excellent throughout all of these observations, and of order 95% or better.

The spectra illustrated in Figs. 2–5 (corresponding to the respective areas A → D in Fig. 1) overlap the less extensive sample of $J=1-0$ spectra presented by Schloerb and Loren (1982), obtained with a somewhat lower spatial (2′) resolution. The consequence, as might be expected, is that whilst agreement is qualitatively close, certain of the spectra show significant differences in profile (cf. 8E 8S), presumably related to the differing beam sizes. This broad correspondence is also to be noted with the more limited sample of overlapping $J=2-1$ ^{13}CO spectra due to Goldsmith et al. (1982) (HPBW = 1′.3), which reveal a similar splitting of the line profiles. It is clear, therefore, that very little (if any) of the line splitting is likely to be due to self-absorption, and

Send offprint requests to: G. J. White

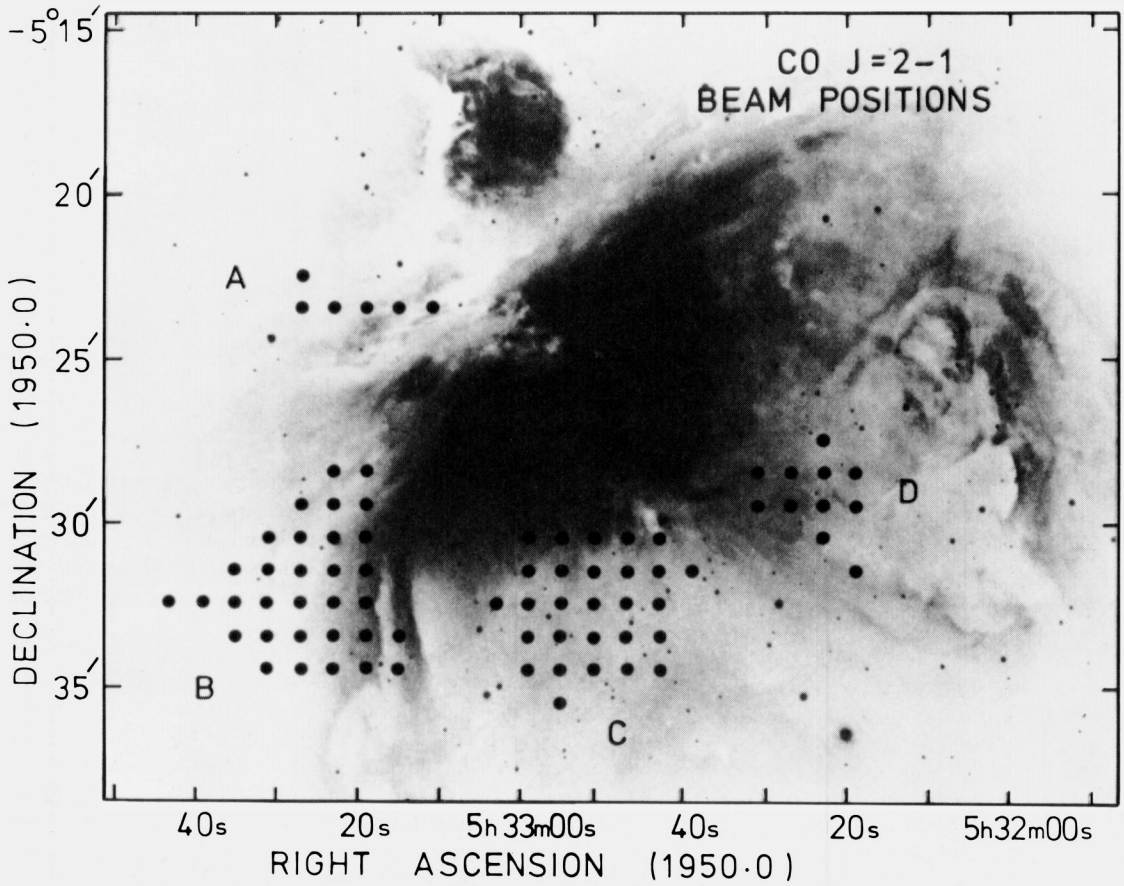

Fig. 1. $J = 2 - 1$ CO beam locations superimposed upon a 6100 Å–7100 Å plate of Orion (Gull, 1974)

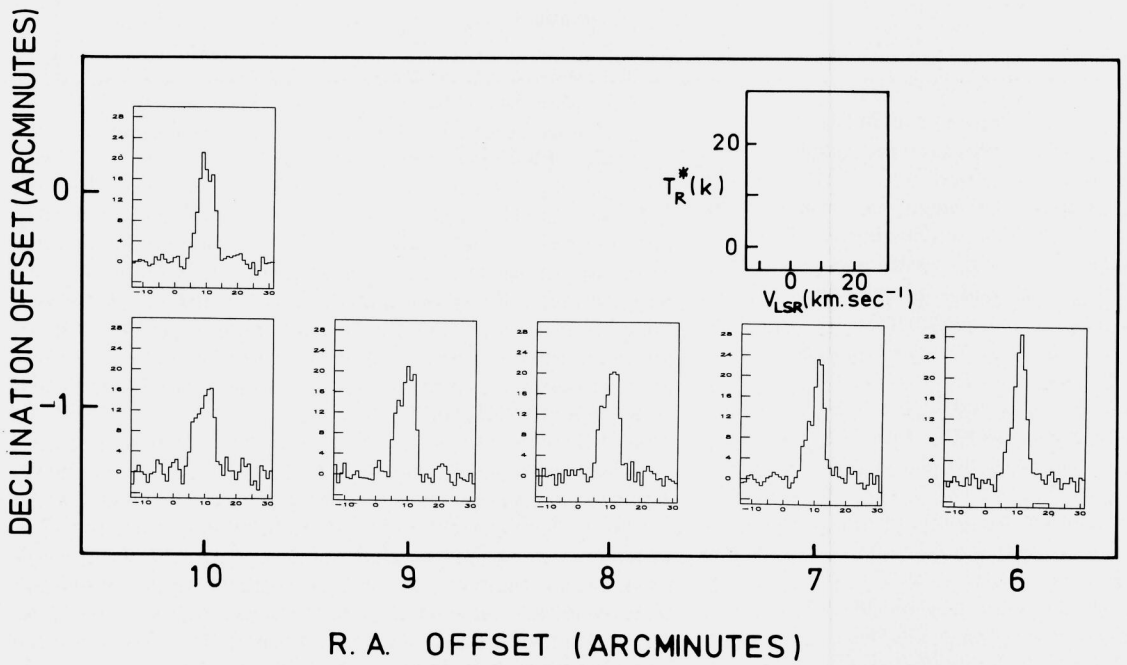

Fig. 2. CO $J = 2 - 1$ spectra for map area A (see Fig. 1). The offset positions are with respect to Ori A ($\alpha = 05^h32^m47^s$; $\delta = -05°24'25''$)

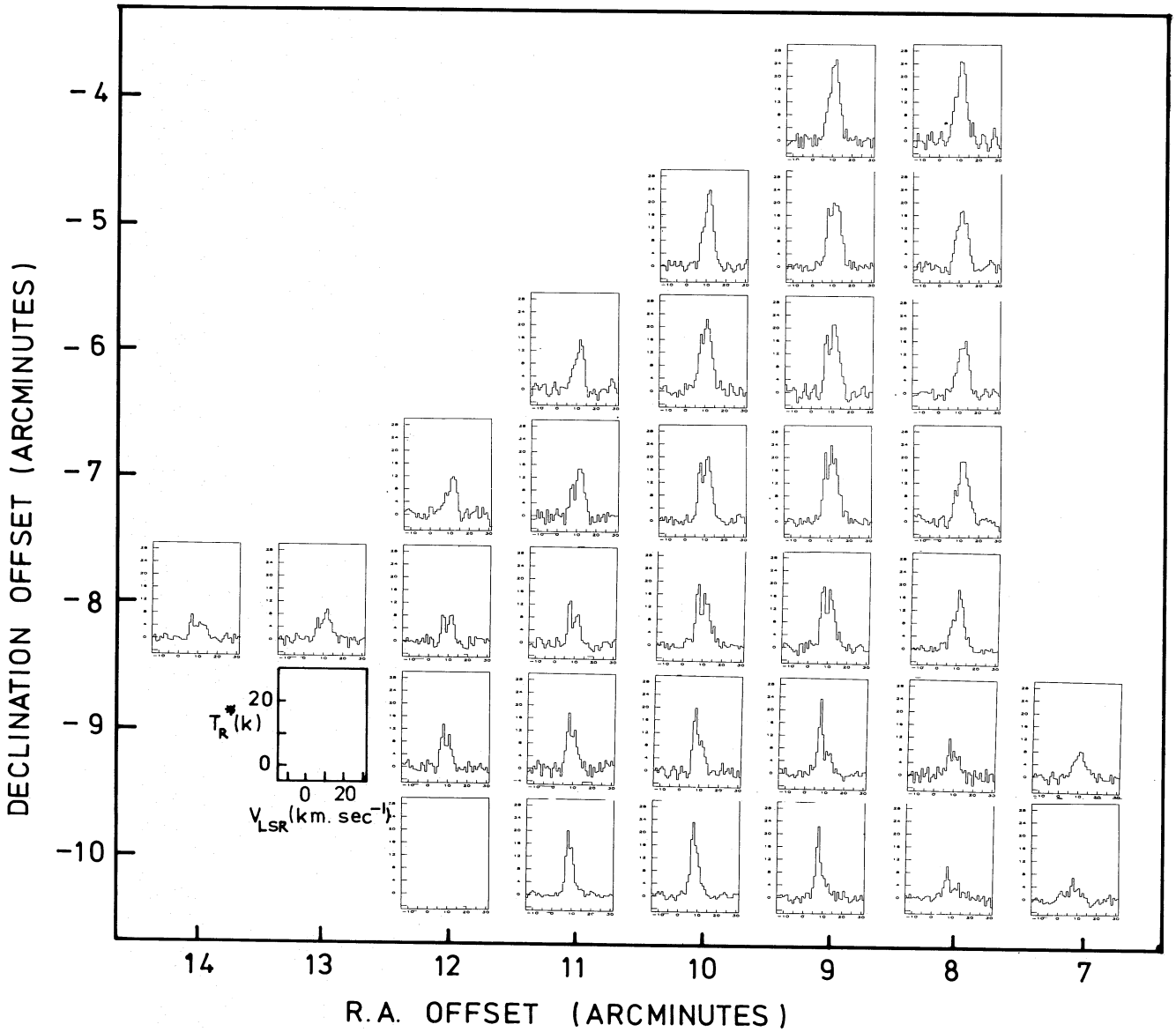

Fig. 3. CO $J = 2 - 1$ spectra for map area B. Otherwise, caption details are as for Fig. 2

our results must reflect the presence of at least two line of sight clouds; one with velocity $\sim 7\,\mathrm{km\,s^{-1}}$, the other at $V_{\mathrm{LSR}} \sim 12\,\mathrm{km\,s^{-1}}$. For the most part, our observations also suggest that there is very little velocity variation over the measured region, although the $12\,\mathrm{km\,s^{-1}}$ component to the south appears to contain a velocity gradient of order $12\,\mathrm{km\,s^{-1}\,pc^{-1}}$ (Fig. 8). This, in turn, leads to a reasonably gentle variation in the apparent separation of the line components (Fig. 4). Finally, we note that the limited comparison with ^{13}CO spectra indicates that relative optical depths vary as between the two primary components. Taking the 9S 9E position as typical, however, and allowing provisos concerning the differing beams employed (although the harmonic mean areas are not dissimilar), we find the optical depths $\tau_{7.3}(^{13}\mathrm{CO}) = -\ln(1 - T_R^*(^{13}\mathrm{CO})/T_R^*(^{12}\mathrm{CO})) \sim 0.6$ at $7.3\,\mathrm{km\,s^{-1}}$, and $\tau_{12}(^{13}\mathrm{CO}) \sim 0.2$ at $12\,\mathrm{km\,s^{-1}}$. Adopting an isotopic ratio $[^{12}\mathrm{C}]/[^{13}\mathrm{C}]$ of ~ 67 (Penzias, 1979), $[12\mathrm{CO}]/[\mathrm{H_2}] \sim 10^{-4}$, excitation temperatures $T_{\mathrm{ex}}(^{13}\mathrm{CO}) \simeq 10\,\mathrm{K}$ at $12\,\mathrm{km\,s^{-1}}$ and 27 K at $7.3\,\mathrm{km\,s^{-1}}$ (based upon peak CO temperatures T_R^*), line widths $\Delta V_{7.3}(^{13}\mathrm{CO}) \simeq 1\,\mathrm{km\,s^{-1}}$ and $\Delta V_{12}(13\mathrm{CO}) = 3.1\,\mathrm{km\,s^{-1}}$, and finally a ratio $A_v/N(\mathrm{H_2}) \simeq 10^{-21}$, it follows that the extinction associated with these components is likely to be modest, and of order $A_v \sim 3.4$ mag at $7.3\,\mathrm{km\,s^{-1}}$, and $A_v \sim 1.3$ mag at $12\,\mathrm{km\,s^{-1}}$.

Such values represent, of course, no more than beam-averaged estimates, and we shall later note that whilst low resolution measures of the optical extinction give similar values for the foreground extinction, higher resolution investigations reveal an extremely complex foreground structure, and very much larger localised extinction. In this respect, we note that appreciable beam dilution $W < 1$ due to CO emission zone clumping would be unlikely to result in a substantial revision of $\tau(^{12}\mathrm{CO})$ – unless the individual clumps possessed appreciable radial density gradients, say. The brightness temperature of the clumps would be of order $T_R^*(^{12}\mathrm{CO})/W$, however, and this would imply a proportionate increase in individual clump extinctions by a factor $\approx W^{-1}$, all other factors being equal. Averaged over the instrumental beam

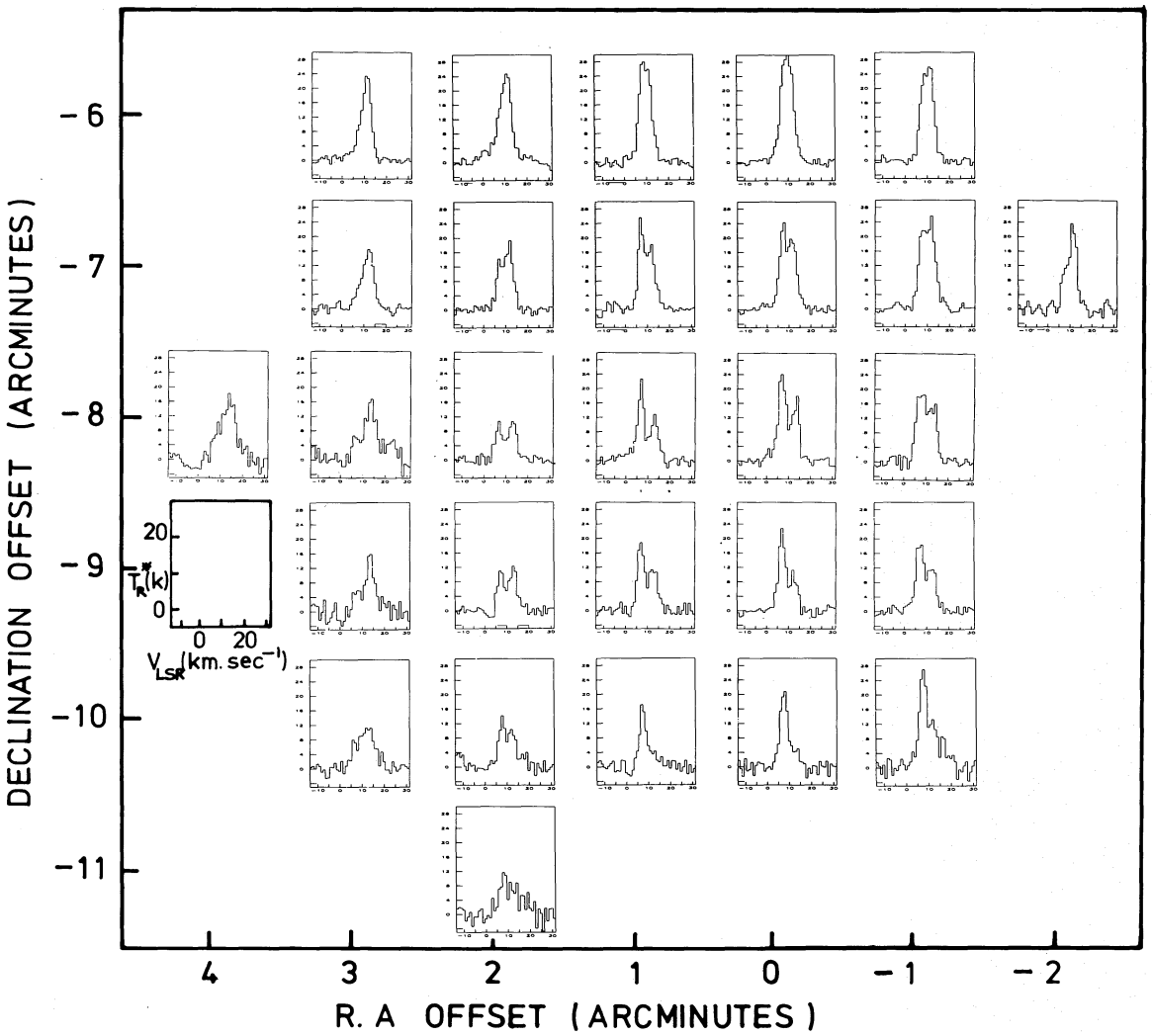

Fig. 4. CO $J = 2 - 1$ spectra for map area C. Caption details otherwise as in Fig. 2

profile, therefore, the mean extinction would be broadly similar to our earlier estimates; the assumption of an inhomogenous emission structure would not greatly alter our conclusions.

Much here depends on the nature of the clumps, if such exist, however, and it is possible to envisage quite differing sets of conclusions; the agreement between observed and theoretical mean extinctions may prove fortuitous. Only more detailed, high resolution measures will clarify this issue.

Finally, the optical depth calculations also assume that LTE applies throughout the region, and that excitation temperatures $T_{ex}(^{13}CO) \sim T_{ex}(CO)$. For local kinetic temperatures $T_k < 30$ K, say, this in turn requires $n(H_2) > 10^4\,cm^{-3}$ for an approximate régime $-6 < \log(X(CO)/dv/dr) < -4\,km\,s^{-1}$ pc, whilst for lower densities, LVG modelling would imply $T_{ex}(CO) > T_{ex}(^{13}CO)$, and values of A_v would be lower than those calculated above. It is clear, therefore, that the estimated extinction $A_v \sim 1.3$ mag for the lesser CO component represents something of an upper limit where densities are $< 10^4\,cm^{-3}$.

Integrated maps of the red and blue velocity components are illustrated in Figs. 6 and 7 for the two primary regions investigated here. It is interesting to note that in both cases, the iso-contours of $\int T_R^*\,dv$ are almost orthogonal; it is apparent that we are dealing with two separate, and not necessarily related clouds. The contours of Fig. 7b in particular show a marked N–S trend, and reveal a strong similarity to the corresponding anterior cloud noted by Loren (1979), associated with the Ori A star formation centre. The $12\,km\,s^{-1}$ component, on the other hand, displays contours which lie parallel to the southern Hβ contours (Fig. 7a), a trend regarded as strong evidence in favour of a compressive post-shock zone (cf. Loren, 1979; Schloerb and Loren, 1982).

The situation at the south-east nebular extremity is less clearly defined; both components have differing spatial distributions, although it would seem that they may both (at least in part) be interpreted as shock configurations. Both sets of contours appear to (weakly) mimic the conformity of the Hβ conpours, for instance, although it is noted that the strongest temperature gradients are located in the $V_{LSR} \sim 12\,km\,s^{-1}$ component, leading to a well defined angular ridge. In either case, it is apparent (from the present data, and that of Loren (1979)) that the presumed post-shock zone must be reasonably extended, and of width $L \sim 3 \rightarrow 4'$. Given that the primary nebular radius R is $\sim 7'$ [cf. the radio map of Schraml and Mezger (1969)], it is plain that the fractional width of the post-shock zone would be of order $L/R \sim 0.5$.

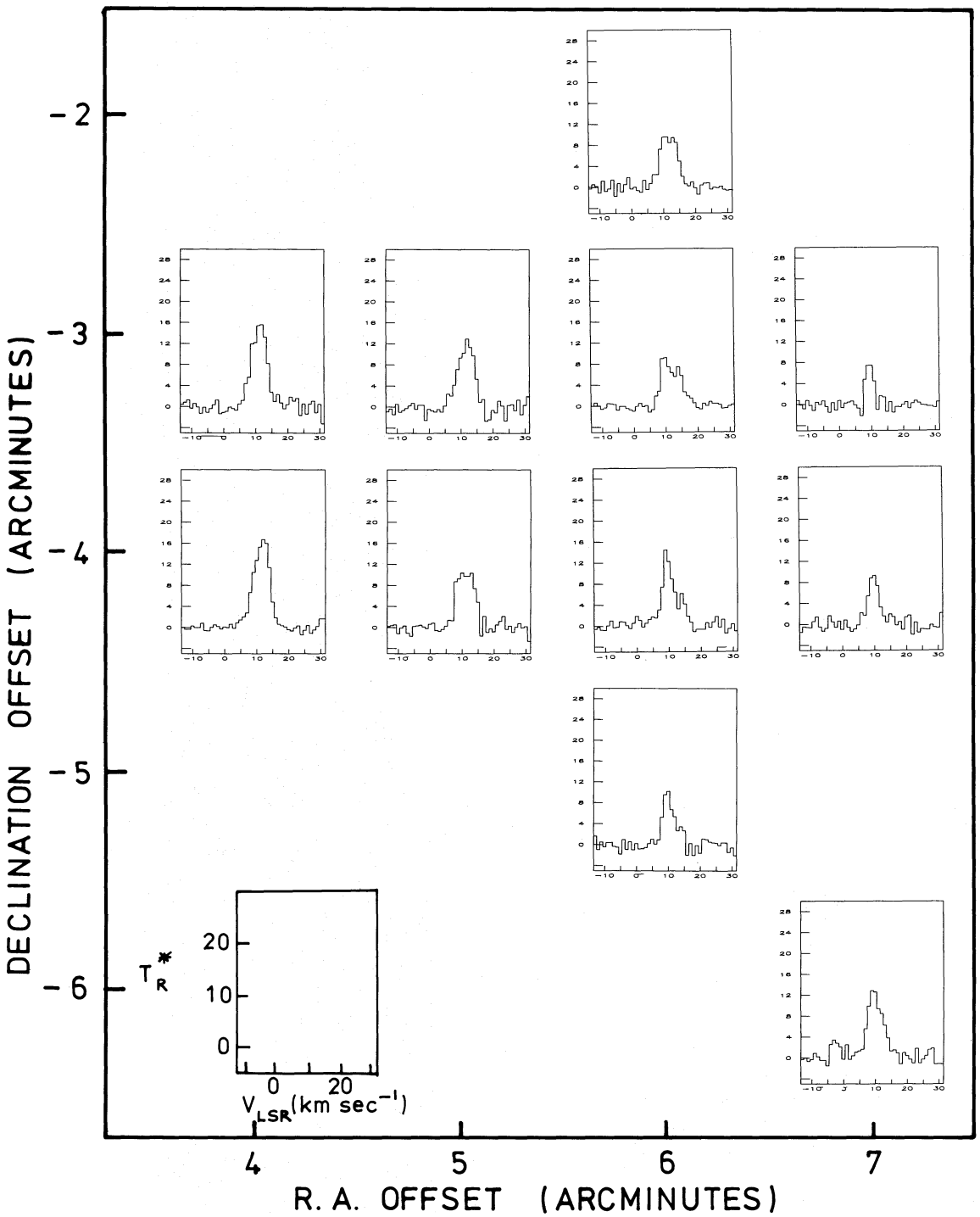

Fig. 5. CO $J = 2 - 1$ spectra for map area D; for caption details see Fig. 2

3. Discussion

On the basis of three primary shock tracers, Schloerb and Loren (1982) argue that the observed line splitting reflects the incursion of pre-cursor shocks into the ambient molecular cloud, ahead of a low velocity ionisation front. In the first place, it is argued that strong [S II] emission is to be expected in post-shock zones, and such filaments are indeed located at the extremities of NGC 1976, where line-splitting is also most evident. It is further claimed that the velocity separation $\Delta V_{\mathrm{LSR}} \approx 4\,\mathrm{km\,s^{-1}}$ between the CO components is consistent with theoretical expectations, as is the width and distribution of the $V_{\mathrm{LSR}} > 9.3\,\mathrm{km\,s^{-1}}$ material.

In the following, we would wish to point out that an alternative hypothesis in terms of unconnected mass components is possible, and may indeed be preferable.

3.1. *Foreground extinction and line splitting*

In the first place, we note that our measurements of multiple kinematic components appear to occur where foregound extinc-

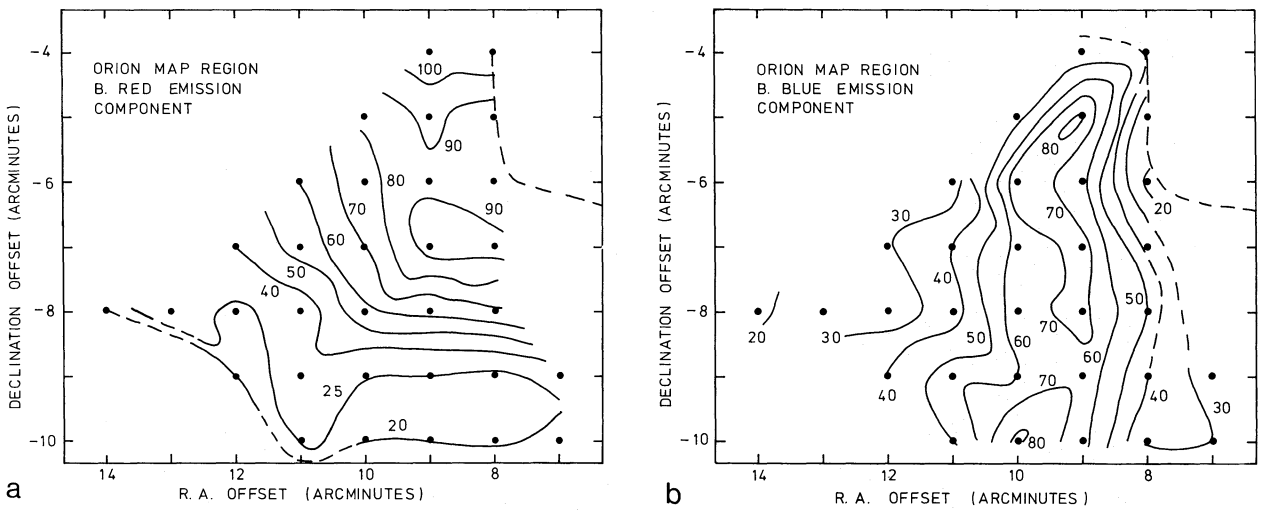

Fig. 6a and b. Integrated fluxes $\int T_R^* \, dv$ (K km s^{-1}) for **a** $V_{LSR} \geqq 9.3$ km s^{-1} (red component) and **b** $V_{LSR} < 9.3$ km s^{-1} (blue component) in map area B. Offsets are given with respect to Ori A, and dots indicate beam locations

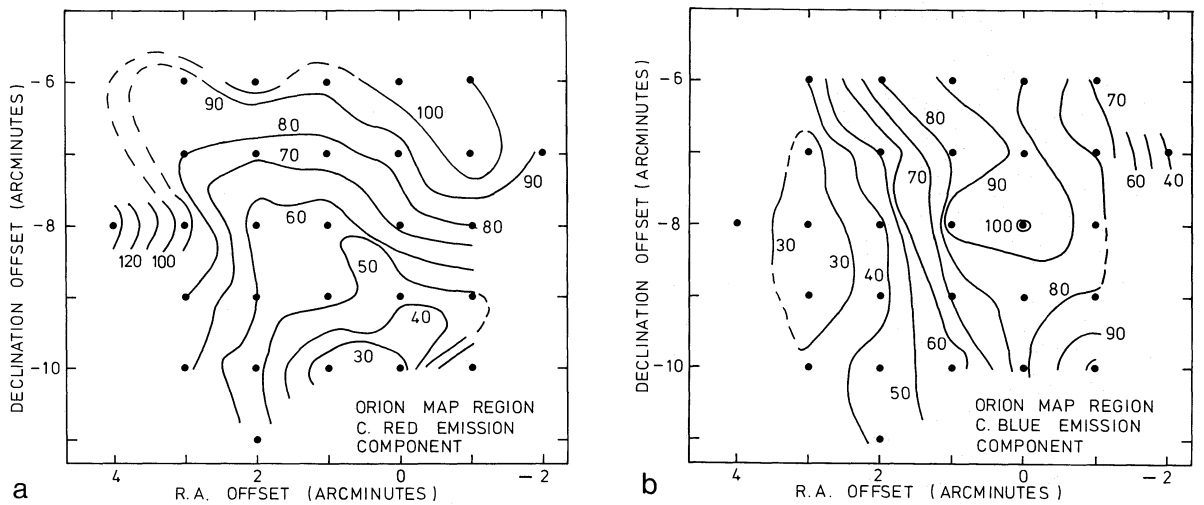

Fig. 7a and b. Integrated fluxes $\int T_R^* \, dv$ (K km s^{-1}) for map area C; caption details are otherwise as for Fig. 6

tion is appreciable. In Fig. 1, for instance, there appears to be clear evidence for a band of extinction across the southerly part of NGC 1976 ($\delta \lesssim -5°30'$), coinciding with the onset of secondary kinematic components in Fig. 3 (see also the narrow band plates in Gull, 1974). Similarly, although low resolution (1.′7) measures of extinction by Chaisson and Dopita (1977) fail to entirely reflect this trend, it is clear that foregound extinction of order $A_v \sim 0.5 \rightarrow 1.0$ mag is distributed across the nebular face; values reasonably similar to those expected of the CO 12 km s^{-1} velocity component (see earlier). Higher resolution (38″) extinction measurements, however, reveal a very much more complex distribution of reddening, and confirm a trend to higher extinction $A_v > 3$ mag towards the south (Barbieri et al., 1976; a pattern also evident in the detailed structure revealed by unsharp masking techniques). Similar trends are also to be noted to the southwest, where CO line splitting occurs in the régime $A_v > 1$ mag, whilst the brighter filamentary zones ($A_v < 0.5$ mag) possess only a single, or at best weak secondary CO component.

There appears to be a clear relationship, in short, between the observed limits of foreground extinction as delineated in optical photographs (cf. Gull, 1974, and the measures of Chaisson and Dopita, 1977, and Barbieri et al., 1976), and the presence of secondary components in the CO spectra indicated here.

3.2. S II *emission zone structure*

A further interesting trend is reflected in the pattern of [S II] emission. The Hα filaments to the southwest of the nebula core, and extending below $\delta \sim -5°28'$, show a distinct morphology in which the eastern extremities are diffuse (and apparently increasingly attenuated by local extinction), whilst the western edges are sharp and well defined (cf. Gull, 1974). It would appear, therefore, that primary ionisation fronts must be proceeding towards the principal ionising sources. (θ^1 Ori A–D, θ^2 Ori A and B), and are presumably encroaching upon the foreground extincting cloud noted above. The [S II] filaments, by way of contrast, display a mottled and rather diffuse structure with no clear-cut boundaries, peaking some way to the rear of the primary I fronts.

This, and the observed Hα structure, might be explainable in a variety of ways; given the observed configuration of the I fronts,

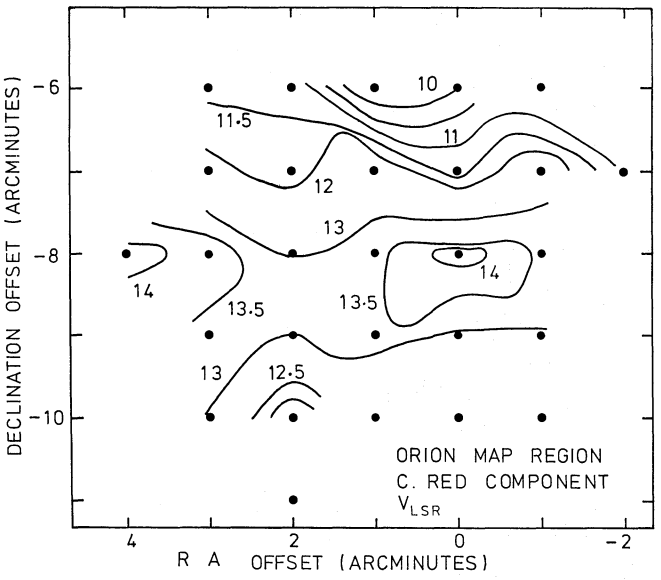

Fig. 8. Variation V_{LSR} (km s^{-1}) for the red component in map C

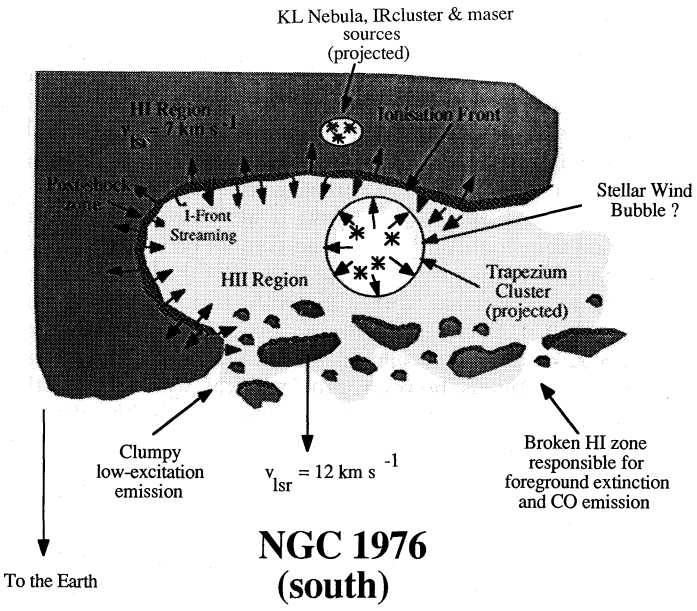

Fig. 9. Schematized view of a southerly cross-section through NGC 1976 with, projected, the relative locations of the more northerly trapezium cluster, and KL nebula

for instance, shadowing from the principal Ly_c source may lead to a low excitation zone, in which primary ionisation arises from secondary photons emerging from the main H II region; a mechanism which would also be expected to result in enhanced [O II] and [N II] components of emission.

Alternatively, we may postulate that the region contains a complex mix of ionised and neutral clumps, perhaps arising from hydrodynamic (Rayleigh-Taylor and Kelvin-Helmholtz) instabilities associated with local I-fronts (cf. Capriotti, 1973). Such clumping would also be expected to result in a wide range of excitations, and a relatively disorganised low-excitation structure.

Finally, of course, it may be possible that secondary O stars are responsible for local excitation, or that [S II] enhancement reflects the local prevalence of shocks (as mentioned earlier). In this latter respect, however, we note that there is little evidence for the sharpedged boundary structures prevailing in higher excitation species (cf. H I, [O III]), and a continuous and clearly defined shock front is apparently absent.

Shock enhancement of [S II] emission through collisional excitation does not, therefore, represent an unique and exclusive interpretation of the observed visual structure of the nebula, and alternative hypotheses in terms of secondary ionisation would be consistent with the observed pattern of extinction, the configuration of the I fronts, and the distribution of CO line splitting.

3.3. Structure of post-shock zones

Finally, we note that the observed ratio $L/R \sim 0.5$ is inconsistent with post-shock widths expected from the modelling of Elmegreen and Lada (1977) – a conclusion at variance with previous analyses of this region. For an H I zone temperature $T_2 \sim 1 (\equiv 10^2$ K), a local density of O stars $N_O \sim 1$ pc^{-3}, and hydrogen number density $n_3 \sim 1$ ($\equiv 10^3$ cm^{-3}; we have used the same parametric definitions as Elmegreen and Lada), for instance, then the separation of the pre-cursor shock and ionisation front takes a value $L/R \sim 4.8\ 10^{-3}$ for a nebular radius $R \sim 1$ pc. These figures may, of course, be massaged somewhat to give a higher value for L/R, although even for $n_3 \sim 10$, and a less plausible $N_O \sim 0.1$, the result ($L/R \sim 0.15$) is barely consistant with the observed width of the line splitting zone.

The apparent magnitude of L/R may of course also be enhanced through hydrodynamics instabilities at (or in advance of) the I front, or alternatively, though the presence of appreciable density contrasts in the ambient medium, both of which processes may lead to an irregular I/shock frontal geometry extending over an appreciable projected depth of material. For this case, however, our CO results suggest that primary deformation must occur over size scales of $\sim 1'$, whilst extending over a radial depth $\sim 3'$; a configuration for which there is little evidence from optical or high resolution radio mapping data. Whether such a mechanism could fully account for the width of the line splitting zone is therefore uncerpain, although a combination of both density contrasts *and* instabilities may well prove significant.

In summary, therefore, we believe that although the line splitting may be interpreted in terms of shock and ambient components of molecular gas at the outer limits of NGC 1976, a plausible (and perhaps more persuasive case) may be made for supposing that the velocity components arise in two separate emission zones; one located to the rear of the H II region, and associated with strong star-forming activity, the other forming a low mean column density, low extinction, and possibly fragmented foreground cloud. A schematic diagram emphasizing the primary characteristics of this model is illustrated in Fig. 9. There is little doubt that compressive I fronts are indeed prevalent in this region, and may be detectable in CO. However, the widths of the post-shock emission zones are likely to be low, and significantly less than the (millimetric) beam sizes obtaining here. More realistic models of shock propogation, on the other hand, in which hydrodynamic instabilities and ambient density contrasts lead to large-scale shock deformation, may well lead to an extended co-spatial region of post- and pre-shock emission.

4. Conclusions

We have presented 77 $J=2-1$ CO spectra of NGC 1976, taken at locations close to the limits of the optical nebulosity. Line splitting is observed over much of these regions, and our results in this respect confirm the $J=1-0$ trends noted by Loren (1979) and others. In particular, two primary velocity components at $V_{LSR} \sim 7\,km\,s^{-1}$ and $V_{LSR} \sim 12\,km\,s^{-1}$ are noted, with radically differing emission distributions and column densities $N(^{13}CO)$; the $7\,km\,s^{-1}$ component arising to the rear of the H II region, and apparently associated with the Ori A star formation zone. Evidence for velocity gradients is also noted in the southerly $V_{LSR} \sim 12\,km\,s^{-1}$ cloud component. The nature of this secondary kinematic feature is, however, problematical, with various other workers arguing for a post-shock zone associated with enhanced, shocked [S II] emission. Our present work suggests, to the contrary, that the $V_{LSR} \sim 12\,km\,s^{-1}$ cloud may represent a foreground feature associated with observed extinction across the face of NGC 1976. The [S II] (and associated Hα) filaments have a peculiar configuration, which is supportive of secondary ionisation by faint, local O stars; clumping to the rear of an I front, perhaps reflective of shock instabilities; or possibly excitation by indirect scattering from the primary H II zone. The distribution of [S II] emission, extinction, and CO line splitting can therefore all be explained in a consistent model, and the shock hypothesis appears unnecessary (and perhaps implausible, given the absence of sharpedged [S II] boundary features). Finally, theoretical models suggest that NGC 1976 may have further to evolve before the neutral post-shock zone takes a width $L \sim 0.5\,R$ characteristic of the observed line splitting zone. Whilst secondary molecular shock components are undoubtedly present at the nebular boundaries, their width is likely to be small, and beam dilution would be high. Alternatively, we must presume that local shock frontal deformation is appreciable, with both hydrodynamic instabilities and ambient density contrasts leading to the apparent mixing of post- and preshock emission.

References

Barbieri, C., Cosmovici, C.B., Michel, K.W., Nishimura, T.: 1976, *Astron. Astrophys.* **47**, 255

Capriotti, E.R.: 1973, *Astrophys. J.* **179**, 495

Chaisson, E.J., Dopita, M.A.: 1977, *Astron. Astrophys.* **56**, 385

Dopita, M.A.: 1978, *Astrophys. J. Suppl.* **33**, 437

Dopita, M.A., Isobe, S., Meaburn, J.: 1975, *Astrophys. Space Sci.* **34**, 91

Elmegreen, B.G., Lada, C.J.: 1977, *Astrophys. J.* **214**, 725

Gillespie, A.R. and White, G.J.: 1980, *Astron. Astrophys.* **91**, 257

Goldsmith, P.F., Arquilla, R., Schloerb, F.P., Scoville, N.Z.: 1982, in *Regions of Recent Star Formation*, eds. R.S. Roger, P.E. Dewdney, D. Reidel Publishing Cô, Dordrecht, Holland, p. 295

Gull, T.R.: 1974, in H II *Regions and the Galactic Centre*, ed. A.F.M. Moorwood, ESRO SP-105

Kutner, M.L., Tucker, K.D., Chin, G., Thaddeus, P.: 1977, *Astrophys. J.* **215**, 521

Loren, R.B.: 1979, *Astrophys. J.* **234**, L 207

Penzias, A.A.: 1979 in *IAU Symp. No.* **83**, ed. B.H. Andrew, D. Reidel Publishing Co., Dordrecht, Holland, p. 181

Schloerb, F.P., Goldsmith, P.F., Scoville, N.Z.: 1982, in *Regions of Recent Star Formation*, eds. R.S. Rogers, P.E. Dewdney, D. Reidel Publishing Co., Dordrecht, Holland, p. 439

Schloerb, F.P., Loren, R.B.: 1982, *Ann. N. Y. Acad. Sci.* **395**, 32

Schraml, J., Mezger, P.G.: 1969, *Astrophys. J.* **156**, 269

White, G.J., Phillips, J.P. Watt, G.D.: 1981, *Monthly Notices Roy. Astron. Soc.* **197**, 745

White, G.J., Monteiro, T.S., Richardson, K.J., Griffin, M.J., Rainey, R.: 1986, *Astron. Astrophys.* **162**, 253